FORSCHUNGSZENTRUM
ROSSENDORF e.V.

FZR

FZR-136
April 1996
Preprint

B. Kämpfer, A. Peshier, M. Hentschel,
G. Soff and O. P. Pavlenko

Electromagnetic signals from deconfined matter resulting from ultrarelativistic heavy-ion collisions

Forschungszentrum Rossendorf e.V.
Postfach 51 01 19 · D-01314 Dresden
Bundesrepublik Deutschland

Telefon (0351) 260 3258
Telefax (0351) 260 3700
E-Mail kaempfer@fz-rossendorf.de

ELECTROMAGNETIC SIGNALS FROM DECONFINED MATTER RESULTING FROM ULTRARELATIVISTIC HEAVY-ION COLLISIONS[a]

B. KÄMPFER[1,2], A. PESHIER[2], M. HENTSCHEL[1], G. SOFF[1]
[1]*Institut für Theoretische Physik, TU Dresden, 01062 Dresden, Germany*
[2]*Forschungszentrum Rossendorf, Institut für Kern- und Hadronenphysik, PF 510119, 01314 Dresden, Germany*

O.P. PAVLENKO
Institute for Theoretical Physics, 252143 Kiev - 143, Ukraine

Electromagnetic radiation off strongly interacting matter resulting from ultrarelativistic heavy-ion collisions is estimated. We consider virtual photons (dileptons) and real photons produced in the course of cooling thermalized matter. The chemical evolution of initially undersaturated parton matter coupled to the longitudinal and transverse expansion is followed. Due to the strong transverse expansion the so-called $M_\perp$ scaling is restored. Some estimates of contributions of the pre-equilibrium stage are presented.

1 Introduction

Electromagnetic signals (leptons and photons) can leave nearly undisturbed a finite system of strongly interacting matter. Therefore, despite of the low production cross sections, the lepton pairs and photons are considered as useful probes of the dynamics of heavy-ion collisions.[1,2] In particular, it is expected that the electromagnetic radiation off highly excited matter, produced in high-energy nuclear collisions, can signalize whether deconfined matter (i.e., the quark-gluon plasma) is transiently created. Unfortunately, there are many sources of dileptons and photons:
(i) Hard first-chance parton collisions produce direct radiation, namely the Drell-Yan yield; in addition, at high beam energies, a copious charm and beauty production is expected, [3,4] which causes via semileptonic decays a strong feeding of the lepton channel.
(ii) The pre-equilibrium contribution is still a matter of debate, but there are some hints that this component might not be negligible (see below).
(iii) What we are mostly interested in is the radiation from thermalized parton (or deconfined) matter.
(iv) The hadronizing parton matter will also radiate electromagnetic signals. Theoretical estimates are still hampered by poor knowledge of the nature of the confinement transition.
(v) Hadronic reactions cause a strong radiation component. A not yet convincingly

[a]Invited talk at International Conference on Nuclear Physics at the Turn of the Millennium, 10 - 16 March, 1996, Wilderness, South Africa.

resolved issue concerns the relation of the yield from this stage to the deconfined matter yield.
(vi) Hadronic decays also contribute substantially to the full spectrum.
This causes problems in unfolding the space-time integrated spectra and in identifying doubtless a possible contribution from deconfined matter. One has therefore to employ sufficiently realistic models of the reaction dynamics in order to estimate the various contributions in different phase space regions.

In the present note we report mainly results of calculations relying on a hydrodynamical evolution scenario for thermalized matter which includes also chemical equilibration processes on the parton level. A few remarks on pre-equilibrium spectra are added.

2 Spectra of dileptons

Details of our dynamical model for thermalized matter are described in reference.[5] In a nut shell: Transverse expansion is superimposed on scale-invariant longitudinal expansion. The transverse expansion is dealt with our global hydrodynamics.[6] Since deconfined matter is predicted to be created in a chemical off-equilibrium state[3,7,8] we follow the evolution of thermalized matter by means of local rate equations. We assume such a fast equilibration that at confinement temperature a chemical equilibrium is reached, and we utilize the standard procedure to follow the confinement transition of hadronizing matter. In the hadronic phase we include the recently proposed effective form factor[9] for describing the dilepton rates. It is assumed that the contributions from the hadronic decays after freeze-out can be subtracted from experimental spectra, so this component is not included in our model. We utilize here a bag model equation of state in the deconfined phase, but we reduce the latent heat by scaling up the effective number of degrees in the hadron phase (see reference[5] for details).

We now present the results of our calculations. The initial conditions for the thermalized era are characterized by the time $\tau_0 = 0.32$ fm/c, temperature $T_0 = 550$ MeV, chemical potential $\mu = 0$, gluon fugacity $\lambda_g^0 = 0.5$ or 0.25, quark fugacity $\lambda_q^0 = \frac{1}{5}\lambda_g^0$ (unless $\lambda_{q,g} = 1$), transverse radius $R_\perp^0 = 7$ fm, transverse velocity $v_\perp^0 = 0$. Fugacity means here phase space occupancy.

2.1 Invariant mass spectra

Figure 1 displays the invariant mass spectrum for all thermal contributions summed and the Drell Yan yield. The latter one is for RHIC conditions ($\sqrt{s} = 200$ GeV) and scaled for central collisions of nuclei with mass number $A = 200$ by $A^{4/3}$; Duke-Owens structure functions, set 1.1 with K factor 2, are used. Figure 1 should be compared with figure 3 in reference,[5] where T_0 is kept fixed. Here we keep the initial entropy or energy density fixed, therefore the actual initial temperatures are $\hat{T}_0 = T_0(\lambda_g^0)^{-1/3}$ or $\hat{T}_0 = T_0(\lambda_g^0)^{-1/4}$. One can observe in figure 1 that indeed the smaller initial fugacity is nearly compensated by the higher temperature. We display here the spectra only in the relevant region up to or slightly above the J/ψ. At much

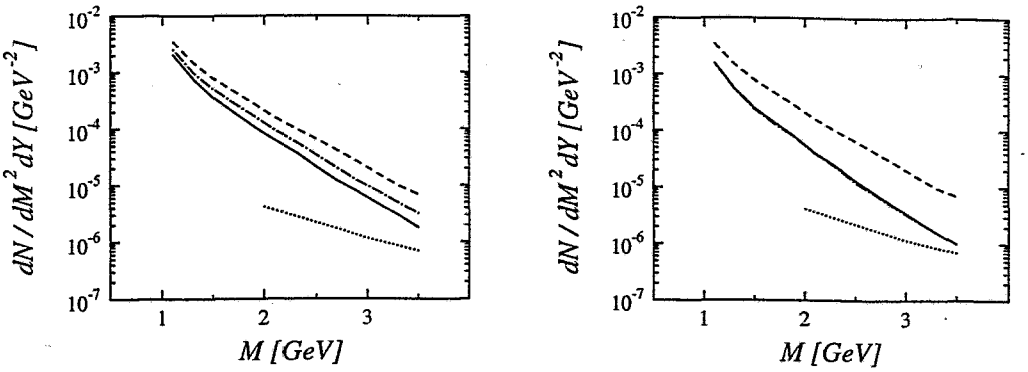

Figure 1: Invariant mass spectra of dileptons for initial temperatures $\hat{T}_0 = T_0(\lambda_g^0)^{-1/3}$ (left panel, corresponding to constant entropy density s_0) and $\hat{T}_0 = T_0(\lambda_g^0)^{-1/4}$ (right panel, corresponding to constant energy density e_0), and $\lambda_q^0 = \frac{1}{5}\lambda_g^0$ when ever $\lambda_g^0 < 1$. The dotted lines depict the Drell Yan background, while the dashed ($\lambda_g^0 = 1$), full ($\lambda_g^0 = 0.5$) and dot-dashed lines ($\lambda_g^0 = 0.25$) display the total yields from the thermal era (parton gas plus mixed phase plus hadron gas).

higher invariant mass, say $M > 10$ GeV, the various curves cross and, despite the lower initial fugacity, the yield related to highest initial temperature (here for $\lambda_g^0 = 0.25$) is largest. So the expectation, [10] that a smaller fugacity is compensated by higher temperature, can be considered as a rough approximation. It should be noticed that the transverse expansion for the given initial temperatures is essential to reduce the life time of the hadron phase, so that the yield from the deconfined stage shines out.

2.2 Transverse momentum spectra

The featureless continuum spectrum does not contain too much information and it seems difficult to read off the underlying dominating radiation source (as demonstrated in reference, [5] a dominating hadron gas source could show structures related to hadronic resonances). Therefore, one should look for other observables. One possibility is to explore peculiarities of the transverse spectra at fixed rapidity Y and fixed transverse mass $M_\perp = \sqrt{M^2 + q_\perp^2}$ as a function of the transverse pair momentum $q_\perp$.

In an initially strongly quark-undersaturated plasma one might expect that the electromagnetic basic process for dilepton production, $q\bar{q} \to \gamma^* \to \mu^+\mu^-$, is not the dominating reaction, but the Compton like reactions $qg \to q\gamma^* \to q\mu^+\mu^-$ and $\bar{q}g \to \bar{q}\gamma^* \to \bar{q}\mu^+\mu^-$ dominate. In figure 2 these yields are displayed together with the other lowest-order α_s annihilation process $q\bar{q} \to g\gamma^* \to g\mu^+\mu^-$. Here the chemical equilibration process is assumed to be fast or slow. Despite the quark undersaturation the electromagnetic annihilation still dominates unless near the kinematical boundary, where the Compton process becomes important. Figure 2 indicates that, for rough estimates, the electromagnetic annihilation within accuracy of factor 2 is sufficient to calculate the rates. Within this accuracy also the $M_\perp$ scaling (i.e., the

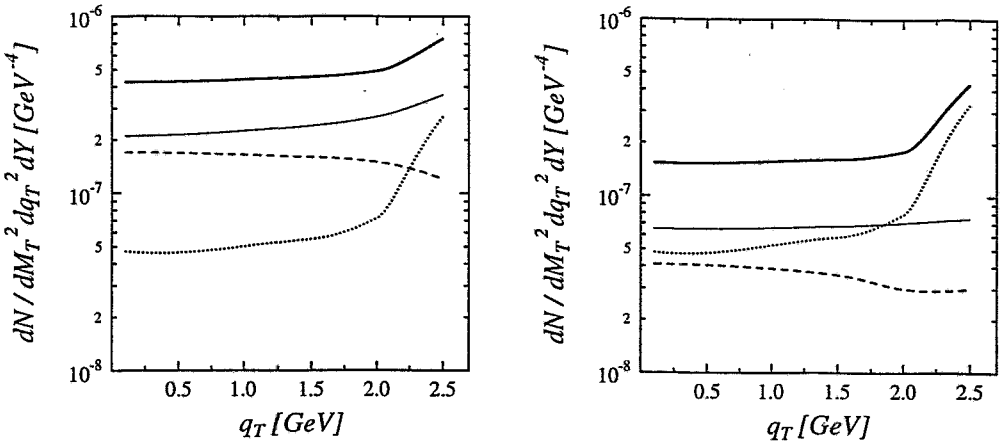

Figure 2: Transverse momentum dilepton spectra for a evolving parton gas with initial conditions $T_0 = 550$ MeV and $\lambda_g^0 = 0.25$; $M_\perp = 2.6$ GeV. The strong coupling parameter is $\alpha_s = 0.3$. Left (right) panel: fast (slow) chemical equilibration is assumed. Thin (dashed, dotted) lines: contributions from the electromagnetic annihilation (QCD annihilation, QCD Compton like) process; heavy full lines: sum of these contributions. This figure should be compared with figure 6 in reference.[5]

$q_\perp$ independence of the spectra with $M_\perp = const$ and $Y = const$) is restored due to the transverse motion, see figure 3. As well known, both the transverse expansion and hadronic form factors usually destroy the $M_\perp$ scaling. However, for the given initial conditions the hadronic era is shortened, so that the dominating deconfinement phase displays as expected the scaling property approximately (cf. however reference[11]).

Notice that regularization procedures of the α_s processes for dileptons radiated off chemical non-equilibrium parton matter need further investigations.[12]

2.3 Rapidity dependence

While the above presented results are for the midrapidity region $Y \approx 0$ and for vanishing chemical potential, one can also explore the rapidity dependence of dileptons from baryon-rich matter.[13] In this respect we refer the interested reader to references.[14,15]

3 Photons

Along the above lines the photon spectra have been calculated.[6] In contrast to the dileptons, these photons, not stemming from hadronic decays, are still searched for. The recent experimental attempts resulted only in upper bounds.[16] One possible way to separate a possible thermal component is to analyze diphotons from the lowest-order process $q\bar{q} \to \gamma\gamma$ and to exclude the hadronic decay products by kinematical cuts. Results of our implementation of the diphoton rates[17] in the above evolution scenario will be presented elsewhere. It should be noticed that the previous WA80 experiment and the present WA93 configuration are so highly segmented that such

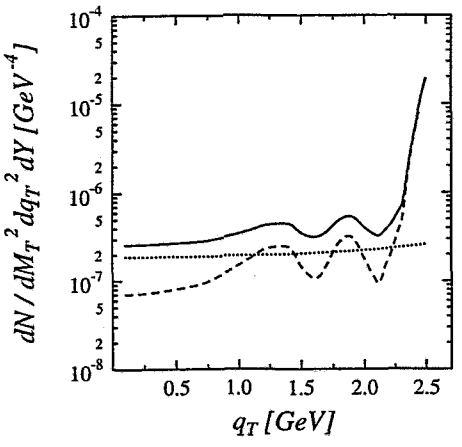

Figure 3: Transverse momentum spectra of dileptons for initial conditions $T_0 = 550$ MeV and $\lambda_q^0 = 0.25$ for $M_\perp = 2.6$ GeV. Dashed (dotted) line: contribution from hadron (parton) gas; full lines: total yields from thermalized matter; fast equilibration is assumed. This figure should be compared with figure 5 in reference. [5]

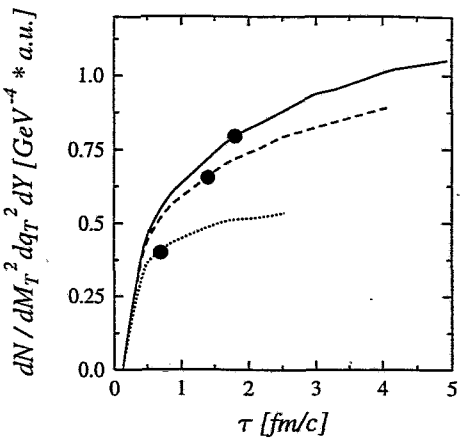

Figure 4: Time evolution of the scaled dilepton spectrum (arbitrary units) from a thermally equilibrating parton gas for invariant mass $M = 2.6$ GeV and transverse momentum $q_\perp = 200$ MeV. The relaxation times are $\tau_{rel} = 10$ fm/c (full line), 1 fm/c (dashed line), 0.13 fm/c (dotted line).

measurements should be easily accessible.

4 Pre-equilibrium dileptons

The recent studies [18,19] point to rather strong contributions from the pre-equilibrium stage, i.e., the time when first-chance collisions had happened and the main part of entropy is produced and the initial coherence of the nuclear parton wave function is destroyed, but the parton distributions does not yet look like a thermal one.

To pin down the relation of the thermal yield and the pre-equilibrium rate we employ here a schematic model. First we display in figure 4 the time evolution of the dilepton yield from a thermally equilibrating parton gas. [18] It is seen that the relaxation time scale influences strongly the yield. The heavy dots indicate the time when roughly 75% of the total yield is produced; obviously this happens within about 25% of the life time of the parton gas.

The solution of the Boltzmann equation in relaxation time approximation has two components

$$f(\tau) = \exp\left\{\frac{\tau_0 - \tau}{\tau_{rel}}\right\} f_0 + \int_{\tau_0}^{\tau} d\tau' \tau_{rel}^{-1} \exp\left\{\frac{\tau_0 - \tau}{\tau_{rel}}\right\} f_{eq}(T(\tau')), \qquad (1)$$

where f is the parton distribution function (assumed to be scale-invariant), τ_{rel} denotes the relaxation time, and f_{eq} stands for the thermal equilibrium distribution function (with temperature parameter T determined by an integral equation, cf. reference [18] for details). Within the kinetic theory framework the dilepton rate has

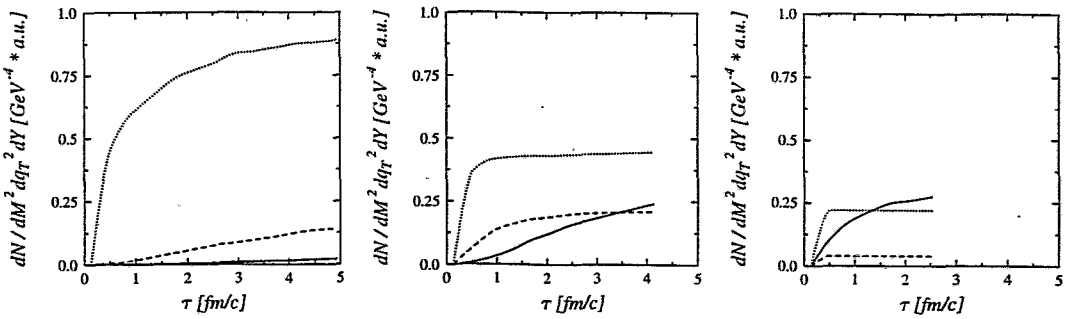

Figure 5: The same as in figure 4, but for the individual contributions: the components N_1, N_2 and N_{12} are depicted by dotted, full, and dashed lines, respectively. The left (middle, right) panel is for the relaxation time τ_{rel} = 10 (1, 0.13) fm/c.

the structure

$$\frac{dN}{d^4x\, d^4Q} = \int \frac{d^3p_1}{2E_1\,(2\pi)^3}\,\frac{d^3p_2}{2E_2\,(2\pi)^3}\,|\mathcal{M}|^2\,(2\pi)^4\,\delta^4(p_1+p_2-Q), \tag{2}$$

with $\mathcal{M}$ for the matrix element of the fusion reaction $q\bar{q} \to \mu^+\mu^-$. Due to the structure of the equation (2) the rate takes the form

$$\frac{dN}{d^4x\, d^4Q} = \int \{\cdots f_0\, f_0 + \cdots f_0\, f_{eq} + \cdots f_{eq}\, f_{eq}\}, \tag{3}$$

i.e., the dileptons are produced by collisions among the non-equilibrated partons ($dN_1 \propto f_0 f_0$), and among the equilibrated ($dN_2 \propto f_{eq} f_{eq}$), and by collisions of non-equilibrated with equilibrated partons ($dN_{12} \propto f_0 f_{eq}$). These three components are displayed in figure 5. Here, as in figure 4, the initial conditions are so that the energy density corresponds to the energy density of an equilibrium system at T = 500 MeV. The initial distribution function f_0 at initial time τ_0 = 0.13 fm/ is chosen as $f_0 \propto \delta(Y-y)\,\exp\{-p_\perp^2/K\}$ with y as space-time rapidity and K = 0.6 GeV^2, cf. [18] One can observe that even for the comparatively short standard equilibration time scale of τ_{rel} = 1fm/c the non-equilibrium component still dominates; only for extremely rapid equilibration the equilibrium component represents the main part in the rate. From this one can conclude that probably the pre-equilibrium dileptons are an important and non-negligible part of the spectrum, despite the short relaxation found in the parton transport simulations.[3,7,8] This holds in particular for the harder dileptons.

5 Summary

In summary we report here mainly estimates of the dilepton spectra to be expected under RHIC conditions, where a substantial part of the transverse energy is produced by perturbative hard or semi-hard QCD processes. Single photon spectra have been calculated within the same dynamical framework.

Acknowledgments

Valuable discussions with K. Redlich are gratefully acknowledged. This work is supported by BMBF (grant 06DR666), DFG and GSI.

References

1. I. Tserruya, *Nucl. Phys.* A **590**, 127c (1995).
2. H.S. Matis and the DLS collaboration, *Nucl. Phys.* A **583**, 617 (1995).
3. P. Levai, B. Müller, X.N. Wang, *Phys. Rev.* C **51**, 3326 (1995).
4. P.L. McGaughey, E. Quack, P.V. Ruuskanen, R. Vogt, X.N. Wang, *Int. J. Mod. Phys.* A **10**, 2999 (1995);
   R. Vogt, preprint LBL-37105 (1996);
   Z. Lin, M. Gyulassy, *Phys. Rev.* C **51**, 2177 (1995).
5. B. Kämpfer, O.P. Pavlenko, A. Peshier, G. Soff, *Phys. Rev.* C **52**, 2704 (1995).
6. B. Kämpfer, O.P. Pavlenko, *Z. Phys.* C **42**, 491 (1994).
7. K. Geiger, *Phys. Rev.* D **46**, 4965 (1992), *Phys. Rev.* D **46**, 4986 (1992), *Phys. Rev.* D **47**, 133 (1992), *Phys. Rev.* D **47**, 4986 (1992);
   K. Geiger, J.I. Kapusta, *Phys. Rev.* D **47**, 4905 (1993).
8. T.S. Biro, E. van Doorn, B. Müller, M.H. Thoma, X.N. Wang, *Phys. Rev.* C **48**, 1275 (1993).
9. D.K. Srivastava, J. Pan, V. Emel'yanov, C. Gale, *Phys. Lett.* B **329**, 157 (1994).
10. E.V. Shuryak, *Phys. Rev. Lett.* **68**, 3270 (1992).
11. B. Kämpfer, O.P. Pavlenko, *Phys. Rev.* C **49**, 2716 (1994).
12. J. Cleymans, I. Dadič, *Phys. Rev.* D **47**, 160 (1993).
13. C. Spieles, M. Bleicher, A. Dumitru, C. Greiner, M. Hofmann, A. Jahns, U. Katscher, R. Matiello, J. Schaffner, H. Sorge, L. Winckelmann, J. Maruhn, H. Stöcker, W. Greiner, *Nucl. Phys.* A **590**, 271c (1995).
14. A. Dumitru, D.H. Rischke, Th. Schönfeld, L. Winckelmann, H. Stöcker, W. Greiner, *Phys. Rev. Lett.* **70**, 2860 (1993);
   A. Dumitru, U. Katscher, J.A. Maruhn, H. Stöcker, W. Greiner, D.H. Rischke, *Z. Phys.* A **353**, 187 (1995), *Phys. Rev.* C **51**, 2166 (1995).
15. B. Kämpfer, O.P. Pavlenko, M.I. Gorenstein, A. Peshier, G. Soff, *Z. Phys.* A **353**, 71 (1995).
16. WA80 collaboration, preprint submitted to *Phys. Rev. Lett.* , (1996).
   T.C. Awes, *Nucl. Phys.* A **590**, 81c (1995).
17. R. Yohida, T. Miyazaki, M. Kadoya, *Phys. Rev.* D **35**, 388 (1987);
   K. Redlich, *Phys. Rev.* D **36**, 3378 (1987);
   S. Hirasawa, M. Kadoya, T. Miyazaki, *Phys. Lett.* B **218**, 263 (1989).
18. B. Kämpfer, O.P. Pavlenko, *Phys. Lett.* B **62**, 127 (1992).
19. K. Geiger, J.I. Kapusta, *Phys. Rev. Lett.* **70**, 1920 (1993);
   K. Geiger, *Phys. Rev. Lett.* **71**, 3075 (1993).